ILKOM Jurnal Ilmiah Vol. 17, No. 3, December 2025, pp. 262-275
Accredited 2nd by RISTEKBRIN No. 10/C/C3/DT.05.00/2025; E-ISSN 2548-7779 | P-ISSN 2087-1716

Prediction of Rice Production in Jember Regency Using Adaptive Neuro Fuzzy Inference System (ANFIS)

Abduh Riski [a,1,*]; Novia Ayu Putriana [a]; Firda Fadri [a]; Ahmad Kamsyakawuni [a]; Agustina Pradjaningsih [a]; Kiswara Agung Santoso [a]; Merysa Puspita Sari [a]
[a] *Department of Mathematics, University of Jember, Jl. Kalimantan No. 37, Jember, 68121, Indonesia*
[1] *riski.fmipa@unej.ac.id,* [2]*putriana2911@gmail.com*
** Corresponding author*

Article history: Received May 24, 2025; Revised August 27, 2025; Accepted November 25, 2025; Available online December 09, 2025

Abstract

Jember Regency is the fourth largest rice-producing regency/city in East Java, so Jember Regency dramatically contributes to increasing the agricultural sector in East Java Province. However, the level of rice production can fluctuate, which is influenced by other factors such as rainfall. A prediction system is needed to anticipate a decrease in rice production. This research aims to predict rice production in the Jember Regency using the Adaptive Neuro Fuzzy Inference System (ANFIS), highlighting the impact of key variables like rainfall, harvested area, and land productivity. This research consists of three stages: training, testing, and prediction. The input variables used in this research are rainfall (mm), harvested area (Ha.), and land productivity (Kw/Ha.), while the output variable is rice production (tons). The membership functions used are generalized Bell and Gaussian, with several combinations of many membership functions. The best model obtained from this research is a model that uses generalized bell membership functions with three membership functions for rainfall variables and two membership functions for harvest area and land productivity variables. The epoch (iteration) used to achieve minimum error is 100 epochs. The best model achieved high accuracy, producing a MAPE value of 0.080% in training and 1.525% in testing, indicating its strong potential for reliable agricultural production forecasting. The predicted amount of rice production in Jember Regency in 2024 was 922,136.8317 tons.

Keywords: ANFIS; Prediction; Rice Production.

Introduction

Jember Regency is a regency that ranks fourth as the largest rice-producing regency/city in East Java in 2021-2023, according to the Badan Pusat Statistik (BPS) of East Java Province [1]. Harvested area [2], [3], land productivity [4], and rainfall [5], [6], [7] influence future rice production. We can use these factors to build a system to predict future rice production. We can use predictions of rice production to detect potential rice shortages and act if the predictions show a significant decrease [8].

We can use the Adaptive Neuro Fuzzy Inference System (ANFIS), which combines artificial neural networks and fuzzy inference systems, as the prediction method [9], [10]. ANFIS works according to IF-THEN fuzzy rules that can learn from the input data [11], [12]. ANFIS applies neural network learning algorithms to adjust automatically adjust parameters and minimize the error between predicted and actual outputs [13], [14].

Some previous research on prediction using the ANFIS method, such as a study predicting rice prices in Lubuklinggau City, has demonstrated its effectiveness, with prediction accuracy results using MAPE of 93.299% for the training process and 88.278% for the testing process [15]. ANFIS has been used in research to predict the volume of waste disposal sites in Samarinda City, and the prediction error using MAPE is 3.36% [16]. ANFIS has also been used to predict monthly rainfall in South Tangerang, with an average accuracy of about 80% during the testing process [17]. ANFIS demonstrated higher accuracy than Multivariable Regression and conventional Artificial Neural Network models in a study predicting the thermal conductivity of water-based MWCNT/ZnO hybrid nanofluids [18]. ANFIS has been effectively used to predict air quality in Semnan, Iran, achieving an R^2 of 0.999 and outperforming models like Multi-Layer Perceptron (MLP) and Random Forest [19]. Similarly, its application in predicting agricultural yields has shown promising results compared to traditional statistical models, which often struggle with the non-linear relationships between variables like weather and crop output [20]. Another previous research used ANFIS to predict sugar production at PTPN XI PG Prajekan, and the results of prediction errors using MAPE were 1.79% in the training

http://dx.doi.org/10.33096/ilkom.v17i3.2797.262-275

process and 4.82% in the testing process [21]. While various machine learning (ML) and deep learning (DL) models exist for agricultural forecasting [22], ANFIS provides a unique advantage by combining the learning capabilities of neural networks with the transparent, rule-based structure of fuzzy logic. This hybrid approach is particularly well-suited for capturing the complex and often imprecise nature of agricultural systems.

This research will predict rice production in the Jember Regency using the ANFIS method. Factors that affect production results, such as harvested area, land productivity, and rainfall, will be used as input variables. The specific contribution of this study is the application and validation of a finely-tuned ANFIS model for rice production in Jember, a key agricultural region, demonstrating a highly accurate (MAPE < 2%) and interpretable alternative to 'black box' ML models. Researchers expect this research to generate a rice production prediction with high accuracy.

Method

A. Research Data

This research uses secondary, time series, and annual data types. Researchers downloaded the data from the official website of the Badan Pusat Statistik (BPS) Jember Regency. The data used are data on rice harvested area (Ha), land productivity (Kw/Ha), rainfall (mm), and rice production (tons) in Jember Regency from 2001-2023. These specific input variables were selected based on established agricultural literature and data availability. Harvested area [2], [3] and land productivity [4] are direct components of total production, while rainfall [5], [6], [7] is a critical, non-linear environmental factor significantly impacting yield, especially in Jember's climate.

B. Adaptive Neuro Fuzzy Inference System (ANFIS)

The Adaptive Neuro Fuzzy Inference System (ANFIS) combines a multi-layer artificial neural network and a first-order Sugeno Fuzzy Inference System (FIS). The rules of the first-order Sugeno model with n inputs and R rules (IF-THEN) are as follows [23].

$$The\ i-th\ rule: IF\ X_1\ is\ A_{1,i}\ AND\ \dots\ AND\ X_n\ is\ A_{n,i}\ THEN\ y_i = \alpha_{0,i} + \alpha_{1,i}X_1 + \cdots + \alpha_{n,i}X_n$$

where $A_{j,i}$ (with $j = 1,2,\dots,n$) is a fuzzy set that represents the linguistic variable in the i-th rule ($i = 1,2,\dots,R$), and $\alpha_{j,i}$ is the consequent parameter.

The ANFIS network has five layers arranged like an artificial neural network. Each layer contains a group of neurons that has interrelated functions with other layers [23], [24]. The explanation of each layer is as follows:

a. Layer 1

Layer 1 is a fuzzification layer that converts input data into membership degrees in fuzzy sets. Equation (1) is the output of layer 1, where i is the number of rules and j is the number of inputs.

$$O_{1,1} = \mu_{A_{j,i}}(X_j) \tag{1}$$

A function approach can determine membership degrees. Membership functions have a common shape, such as a bell shape [26]. The membership functions used in this research are as follows:

1. Generalized bell membership function

$$\mu(x) = \frac{1}{1 + \left|\frac{x-c}{a}\right|^{2b}} \tag{2}$$

where a is a parameter that indicates the curve's width, b is a parameter that affects the slope of the curve, and c is a parameter that determines the position of the center of the curve.

2. Gaussian membership function

$$\mu(x) = e^{-\frac{1}{2}\left(\frac{x-c}{\sigma}\right)^2} \tag{3}$$

where σ is a parameter that indicates the standard deviation of the curve, and c is a parameter that indicates the position of the center of the curve.

The generalized Bell and Gaussian membership functions are used in this study due to their flexibility and smoothness. The generalized Bell function offers high flexibility with three parameters (a, b, c) allowing it to

adjust the width, slope, and center, making it adept at fitting complex data patterns. The Gaussian function, defined by two parameters (σ, c), is a smooth, non-zero function that provides a stable and efficient gradient for the backpropagation algorithm during training [26]. The appropriate selection of membership function number and type is required for accurately representing the input parameters' behavior and complexity [27].

b. Layer 2

Layer 2 is the rules layer. The neurons in this layer are labeled with $\prod$ whose output is the product of the incoming signals. Each neuron in this layer represents the firing strength (w_i) of the i-th rule. Equation (4) is the output of layer 2.

$$O_{2,i} = w_i = \prod_{j=1}^{n} \mu_{A_{j,i}}(X_j) \tag{4}$$

c. Layer 3

Layer 3 is the firing strength normalization layer. We label the neurons in this layer with N. Equation (5), the output of layer 3, where i is the number of rules.

$$O_{3,i} = \bar{w}_i = \frac{w_i}{\sum_{i=1}^{R} w_i} \tag{5}$$

d. Layer 4

Layer 4 is a defuzzification that converts the $O_{3,i}$ value into a numerical value by multiplying the neuron function. Equation (6) is the output of layer 4 where $\bar{w}_i$ s the output of layer 3 and $\{\alpha_{0,i}, \alpha_{1,i}, \ldots, \alpha_{n,i}\}$ are the consequence parameters.

$$O_{4,i} = \bar{w}_i y_i = \bar{w}_i(\alpha_{0,i} + \alpha_{1,i}X_1 + \cdots + \alpha_{n,i}X_n) \tag{6}$$

e. Layer 5

Layer 5 is a single neuron result layer labeled with $\sum$. This layer calculates the overall output as the sum of all incoming signals. Equation (7) is the output of layer 5.

$$O_{5,1} = \sum_{i=1}^{R} \bar{w}_i y_i = \frac{\sum_i w_i y_i}{\sum_i w_i} \tag{7}$$

C. Mean Absolute Percentage Error (MAPE)

Mean Absolute Percentage Error (MAPE) can evaluate the number of prediction errors in ANFIS method. MAPE measurement is easier to understand because it provides an evaluation in the form of percent [27], [28]. The smaller the MAPE value produced, the better the prediction results [29], [30]. MAPE shows the percentage of prediction output error against the actual value in a certain period [32]. Equation (8) is the MAPE calculation formula where Y_t is the actual data in the t-th year, $\hat{Y}_t$ is the predicted data in the t-th year, and n is the number of periods [33].

$$MAPE = \frac{\sum_{t=1}^{n} \frac{|Y_t - \hat{Y}_t|}{Y_t} \times 100\%}{n} \tag{8}$$

Results and Discussion

A. ANFIS Prediction System

The prediction system generates rice production output for the next year using the current year's input variables. The input variables in this research are rainfall in the t-th year $(X_{1,t})$, a harvested area in the t-th year $(X_{2,t})$, and productivity in the t-th year $(X_{3,t})$. In contrast, the output variable in this research is rice production $(t+1)$-th year (Y_{t+1}). The system comprises three stages: the training stage, the testing stage, and the prediction stage.

1. Training Stage

The training stage uses data from 2001-2019 to predict rice production in 2002-2020. The training stage starts with inputting patterns to be trained. At this stage there will be changes in the weights of the membership curve parameters and consequent parameters. The explanation of each layer of the ANFIS network in the training stage is as follows.

a. Layer 1

Layer 1 is the fuzzification layer, so the output of this layer is the membership degree value (μ). Researchers select the combination of membership functions from several experiments that yield low Mean Absolute Percentage Error (MAPE) values during the research phase. **Table 1** shows the combination of trials conducted with 100 epochs.

Table 1. Combination of Research Membership Functions

Membership Functions			MAPE Results	
$X_{1,t}$	$X_{2,t}$	$X_{3,t}$	*Generalized Bell*	*Gaussian*
2	2	2	0.005%	0.038%
2	3	3	0.164%	0.015%
3	2	2	0.019%	0.047%
3	3	3	0.048%	0.017%
4	3	3	0.057%	0.043%

Based on (2) and (3), we initialize the parameters of the membership function curve for three membership functions of variable $X_{1,t}$ and two each for variables $X_{2,t}$ and $X_{3,t}$, as shown in **Table 2**. This parameter initialization determines the shape and position of the membership function to be used. **Figure 1** and **Figure 2** display the visualization of the membership function plot.

Table 2. Training Stage Input Membership Function Parameters

Variable	Membership Degree	Generalized Bell			Gaussian	
		a	b	c	σ	c
$X_{1,t}$	$\mu_{A_{1,1}}$	32.69	2.36	105.685	27.681	105.631
	$\mu_{A_{1,2}}$	32.62	1.88	171.049	27.702	171.027
	$\mu_{A_{1,3}}$	32.67	2.11	236.358	27.745	236.360
$X_{2,t}$	$\mu_{A_{2,1}}$	17328.5	2.08	131522.0	14717.4	131522.0
	$\mu_{A_{2,2}}$	17328.5	1.29	166179.0	14717.4	166179.0
$X_{3,t}$	$\mu_{A_{3,1}}$	6.44	1.34	48.345	8.442	49.581
	$\mu_{A_{3,2}}$	8.45	2.25	61.575	7.329	60.446

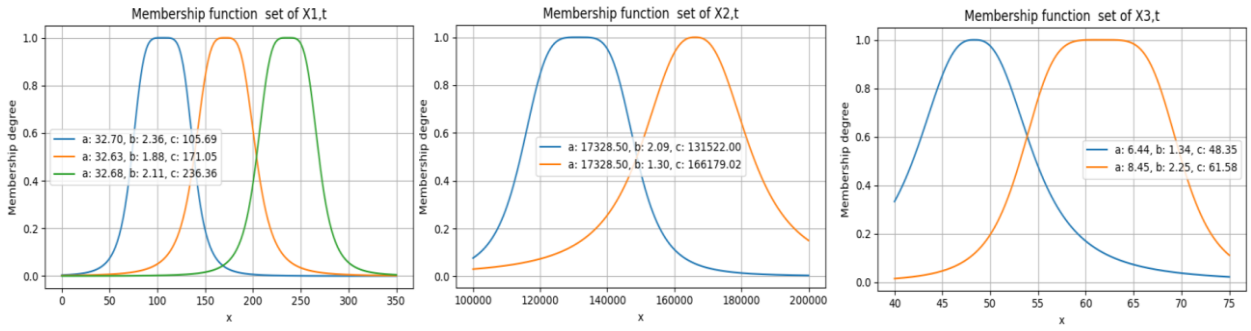

(a) $X_{1,t}$ (b) $X_{2,t}$ (c) $X_{3,t}$

Figure 1. The Plot of Generalized Bell Membership Function Curves

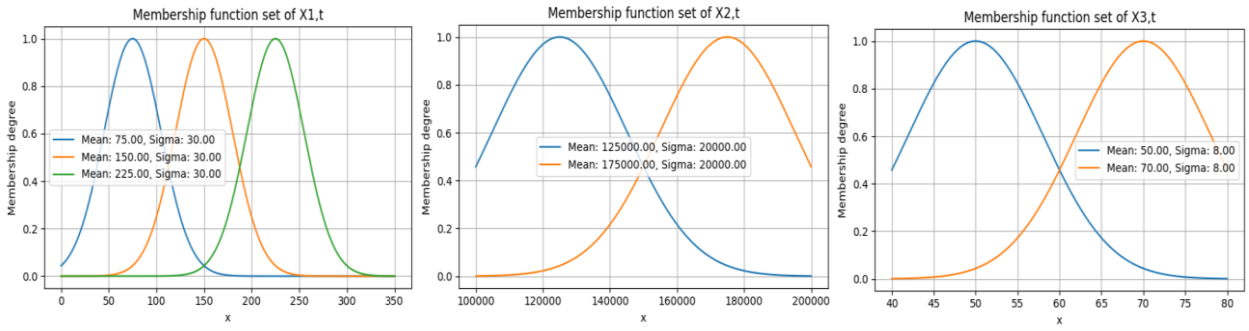

(a) $X_{1,t}$ (b) $X_{2,t}$ $X_{3,t}$

Figure 2. The Plot of Gaussian Membership Function Curves

Output layer 1 with three membership functions for variable $X_{1,t}$ and two membership functions for variables $X_{2,t}$ and $X_{3,t}$ are shown in **Table 3** and **Table 4**.

Table 3. Output Layer 1 Generalized Bell Membership Function (Training Stage)

$X_{1,t}$			$X_{2,t}$		$X_{3,t}$	
$\mu_{1,1}$	$\mu_{1,2}$	$\mu_{1,3}$	$\mu_{2,1}$	$\mu_{2,2}$	$\mu_{3,1}$	$\mu_{3,2}$
0.4662	0.5266	0.0100	0.8367	0.3253	0.9758	0.1966
0.0630	0.9960	0.0329	0.8952	0.2933	0.6297	0.5757
⋮	⋮	⋮	⋮	⋮	⋮	⋮
0.0475	0.9997	0.0409	0.0828	0.9807	0.1778	0.9967
0.0415	0.3411	0.7093	0.0649	0.9971	0.1511	0.9940
0.9999	0.0680	0.0028	0.1592	0.8519	0.0754	0.9988

Table 4. Output Layer 1 Gaussian Membership Function (Training Stage)

$X_{1,t}$			$X_{2,t}$		$X_{3,t}$	
$\mu_{1,1}$	$\mu_{1,2}$	$\mu_{1,3}$	$\mu_{2,1}$	$\mu_{2,2}$	$\mu_{3,1}$	$\mu_{3,2}$
0.4765	0.5197	0.0022	0.7286	0.2965	0.9998	0.6642
0.1119	0.9643	0.0319	0.7806	0.2559	0.9155	0.8840
⋮	⋮	⋮	⋮	⋮	⋮	⋮
0.0834	0.9911	0.0452	0.1113	0.9668	0.5856	0.9925
0.0008	0.3734	0.6347	0.0828	0.9924	0.5356	0.9790
0.9999	0.0617	1.5×10^{-5}	0.2145	0.8315	0.3203	0.8349

b. Layer 2

Layer 2 is a layer that multiplies the membership degrees between inputs according to the rules. The combination of each membership degree of each input derives the number of rules. So, the more membership degrees used, the more rules are formed. The rules formed from three membership functions for variable $X_{1,t}$ and two membership functions for variables $X_{2,t}$ and $X_{3,t}$ can be seen in **Table 5**. The output of layer 2, which is the firing strength of each rule($w_{i,t}$), can be seen in **Table 6** and **Table 7**.

Table 5. Rules of the Membership Function

Rules
IF ($X_{1,t}$ is $A_{1,1}$) AND ($X_{2,t}$ is $A_{2,1}$) AND ($X_{3,t}$ is $A_{3,1}$) THEN (*output is* $w_{1,t}$)
IF ($X_{1,t}$ is $A_{1,1}$) AND ($X_{2,t}$ is $A_{2,1}$) AND ($X_{3,t}$ is $A_{3,2}$) THEN (*output is* $w_{2,t}$)
IF ($X_{1,t}$ is $A_{1,1}$) AND ($X_{2,t}$ is $A_{2,2}$) AND ($X_{3,t}$ is $A_{3,1}$) THEN (*output is* $w_{3,t}$)
IF ($X_{1,t}$ is $A_{1,1}$) AND ($X_{2,t}$ is $A_{2,2}$) AND ($X_{3,t}$ is $A_{3,2}$) THEN (*output is* $w_{4,t}$)
IF ($X_{1,t}$ is $A_{1,2}$) AND ($X_{2,t}$ is $A_{2,1}$) AND ($X_{3,t}$ is $A_{3,1}$) THEN (*output is* $w_{5,t}$)
IF ($X_{1,t}$ is $A_{1,2}$) AND ($X_{2,t}$ is $A_{2,1}$) AND ($X_{3,t}$ is $A_{3,2}$) THEN (*output is* $w_{6,t}$)

Rules
IF ($X_{1,t}$ is $A_{1,2}$) AND ($X_{2,t}$ is $A_{2,2}$) AND ($X_{3,t}$ is $A_{3,1}$) THEN (*output is* $w_{7,t}$)
IF ($X_{1,t}$ is $A_{1,2}$) AND ($X_{2,t}$ is $A_{2,2}$) AND ($X_{3,t}$ is $A_{3,2}$) THEN (*output is* $w_{8,t}$)
IF ($X_{1,t}$ is $A_{1,3}$) AND ($X_{2,t}$ is $A_{2,1}$) AND ($X_{3,t}$ is $A_{3,1}$) THEN (*output is* $w_{9,t}$)
IF ($X_{1,t}$ is $A_{1,3}$) AND ($X_{2,t}$ is $A_{2,1}$) AND ($X_{3,t}$ is $A_{3,2}$) THEN (*output is* $w_{10,t}$)
IF ($X_{1,t}$ is $A_{1,3}$) AND ($X_{2,t}$ is $A_{2,2}$) AND ($X_{3,t}$ is $A_{3,1}$) THEN (*output is* $w_{11,t}$)
IF ($X_{1,t}$ is $A_{1,3}$) AND ($X_{2,t}$ is $A_{2,2}$) AND ($X_{3,t}$ is $A_{3,2}$) THEN (*output is* $w_{12,t}$)

Table 6. Output Layer 2 Generalized Bell Membership Function (Training Stage)

$w_{1,t}$	$w_{2,t}$	$w_{3,t}$	⋯	$w_{10,t}$	$w_{11,t}$	$w_{12,t}$
3.8×10^{-1}	7.6×10^{-2}	1.4×10^{-1}	⋯	1.6×10^{-3}	3.1×10^{-3}	6.4×10^{-4}
3.5×10^{-2}	3.2×10^{-2}	1.1×10^{-2}	⋯	1.6×10^{-2}	6.0×10^{-3}	5.5×10^{-3}
⋮	⋮	⋮	⋮	⋮	⋮	⋮
7.0×10^{-4}	3.9×10^{-3}	8.3×10^{-3}	⋯	3.3×10^{-3}	7.1×10^{-3}	3.9×10^{-2}
4.0×10^{-5}	2.6×10^{-4}	6.2×10^{-4}	⋯	4.6×10^{-2}	1.0×10^{-1}	7.0×10^{-1}
1.2×10^{-2}	1.5×10^{-1}	6.4×10^{-2}	⋯	4.5×10^{-4}	1.8×10^{-4}	2.4×10^{-3}

Table 7. Output Layer 2 Gaussian Membership Function (Training Stage)

$w_{1,t}$	$w_{2,t}$	$w_{3,t}$	⋯	$w_{10,t}$	$w_{11,t}$	$w_{12,t}$
3.4×10^{-1}	2.3×10^{-1}	1.4×10^{-1}	⋯	1.0×10^{-3}	6.5×10^{-4}	4.3×10^{-4}
7.9×10^{-2}	7.7×10^{-2}	2.6×10^{-2}	⋯	2.2×10^{-2}	7.4×10^{-3}	7.2×10^{-3}
⋮	⋮	⋮	⋮	⋮	⋮	⋮
1.9×10^{-4}	3.5×10^{-4}	2.3×10^{-3}	⋯	3.0×10^{-2}	2.0×10^{-1}	3.5×10^{-1}
3.6×10^{-5}	6.7×10^{-5}	4.4×10^{-4}	⋯	5.1×10^{-2}	3.3×10^{-1}	6.1×10^{-1}
6.8×10^{-2}	1.7×10^{-1}	2.6×10^{-1}	⋯	2.7×10^{-6}	4.0×10^{-6}	1.0×10^{-5}

c. Layer 3

Layer 3 is a layer that normalizes the firing strength from layer 2. We calculate normalization by dividing the firing strength of each rule by the total firing strength. The output of layer 3 can be seen in **Table 8** and **Table 9**.

Table 8. Output Layer 3 Generalized Bell Membership Function (Training Stage)

$\bar{w}_{1,t}$	$\bar{w}_{2,t}$	$\bar{w}_{3,t}$	⋯	$\bar{w}_{10,t}$	$\bar{w}_{11,t}$	$\bar{w}_{12,t}$
2.7×10^{-1}	5.6×10^{-2}	1.0×10^{-1}	⋯	1.2×10^{-3}	2.3×10^{-3}	4.7×10^{-4}
2.2×10^{-2}	2.0×10^{-2}	7.4×10^{-3}	⋯	1.0×10^{-2}	3.8×10^{-3}	3.5×10^{-3}
⋮	⋮	⋮	⋮	⋮	⋮	⋮
5.1×10^{-4}	2.8×10^{-3}	6.1×10^{-3}	⋯	2.4×10^{-3}	5.2×10^{-3}	2.9×10^{-2}
3.1×10^{-5}	2.0×10^{-4}	4.8×10^{-4}	⋯	3.5×10^{-2}	8.2×10^{-2}	5.4×10^{-1}
1.0×10^{-2}	1.3×10^{-1}	5.5×10^{-2}	⋯	3.9×10^{-4}	1.5×10^{-4}	2.1×10^{-3}

Table 9. Output Layer 3 Gaussian Membership Function (Training Stage)

$\bar{w}_{1,t}$	$\bar{w}_{2,t}$	$\bar{w}_{3,t}$	⋯	$\bar{w}_{10,t}$	$\bar{w}_{11,t}$	$\bar{w}_{12,t}$
2.0×10^{-1}	1.3×10^{-1}	8.2×10^{-2}	⋯	6.2×10^{-4}	3.8×10^{-4}	2.5×10^{-4}
3.8×10^{-2}	3.7×10^{-2}	1.2×10^{-2}	⋯	1.0×10^{-2}	3.6×10^{-3}	3.5×10^{-3}
⋮	⋮	⋮	⋮	⋮	⋮	⋮
2.8×10^{-3}	4.8×10^{-3}	2.4×10^{-2}	⋯	2.6×10^{-3}	1.3×10^{-2}	2.2×10^{-2}
2.2×10^{-5}	4.0×10^{-5}	2.6×10^{-4}	⋯	3.1×10^{-2}	2.0×10^{-1}	3.7×10^{-1}
5.3×10^{-2}	1.3×10^{-1}	2.0×10^{-1}	⋯	2.1×10^{-6}	3.1×10^{-6}	8.2×10^{-6}

d. Layer 4

Layer 4 is the defuzzification layer, where the output of layer 3 will be multiplied by the consequent parameter. In the Python script, there is a trainHybridJangOffline function [34]. The function has a loop command that will run when the epoch value has not reached the specified epoch value, and the error value is less than the tolerance error value. This layer also changes the membership curve parameters and consequent parameters. Membership curve parameters are updated using backpropagation error, while consequent parameters are calculated using a recursive Least Square Estimator (LSE). The number of epochs influences the error results at each iterations, so it is necessary to determine the right epoch to get a good error value to avoid underfitting or overfitting the model. **Table 10** shows the MAPE values of three membership functions for variable $X_{1,t}$ and two membership functions for variables $X_{2,t}$ and $X_{3,t}$ with different epochs. The consequent parameters with 100 epochs are shown in **Table 11**.

Table 10. MAPE Results with Various Epochs

Epoch	Generalized Bell	Gaussian
100	0.0192%	0.0475%
200	0.0379%	0.0677%
300	0.0333%	0.0834%

Table 11. Result of Layer 4 Consequent Parameters

Consequent Parameter	Generalized Bell	Gaussian
$\alpha_{0,1}$	-1.803×10^{1}	-9.3835×10^{1}
$\alpha_{1,1}$	-5.454×10^{2}	1.0587×10^{4}
$\alpha_{2,1}$	7.244×10^{0}	-1.5208×10^{1}
$\alpha_{3,1}$	-1.084×10^{3}	-4.0516×10^{3}
⋮	⋮	⋮
$\alpha_{0,12}$	-1.071×10^{1}	-1.1792×10^{2}
$\alpha_{1,12}$	2.107×10^{3}	1.7925×10^{4}
$\alpha_{2,12}$	4.013×10^{0}	-1.0190×10^{1}
$\alpha_{3,12}$	-1.071×10^{1}	-8.1332×10^{3}

Plots that show the MAPE errors at each iteration of three membership functions for variable $X_{1,t}$ and two membership functions for variables $X_{2,t}$ and $X_{3,t}$ with 100 epochs can be seen in **Figure 3**.

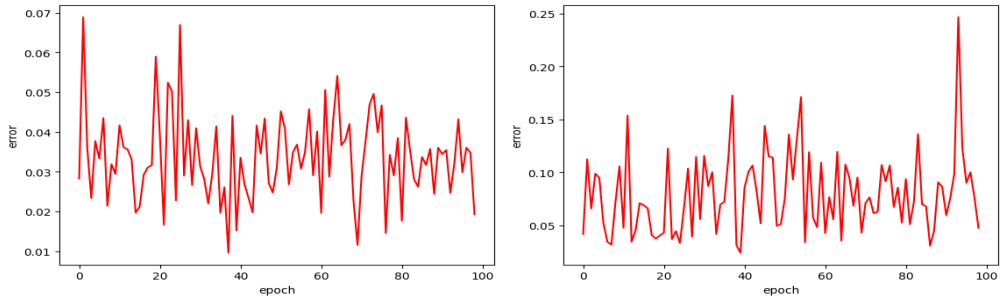

(a) Generalized Bell (b) Gaussian

Figure 3. MAPE Plot of Generalized Bell and Gaussian Membership Function

e. Layer 5

Layer 5 is the layer that sums up the results of Layer 4. Table 12shows the output of layer 5 from three membership functions for variable $X_{1,t}$ and two membership functions for variables $X_{2,t}$ and $X_{3,t}$ along with the actual data. **Figure 4** is a plot that visualizes the actual data and prediction data from the ANFIS training. The plot shows that the predicted data has a very similar value to the actual data because the red line representing the predicted data overlaps with the blue line representing the actual data.

Table 12. Training Stage Results

Year (t)	Actual Data (t + 1)	Prediction Data (t + 1)	
		Generalized bell	*Gaussian*
2001	704282	703928.544	704630.016
2002	761523	761466.680	761376.195
2003	720774	720872.470	720566.711
2004	739744	739773.194	739721.321
2005	749243	749187.049	748996.432
2006	773786	775382.118	776099.237
2007	813995	813845.739	813894.250
2008	880750	880430.958	880529.751
2009	845094	844685.321	845645.909
2010	830000	829123.418	828916.484
2011	970096	969837.407	969780.627
2012	930027	930409.809	929724.239
2013	978373	978115.531	976742.896
2014	1004898	1004468.987	1005148.133
2015	986653	984536.132	987081.638
2016	960602	958047.525	961790.984
2017	984201	984527.659	984061.887
2018	997838	996209.908	998528.007
2019	991892	989767.663	992751.693

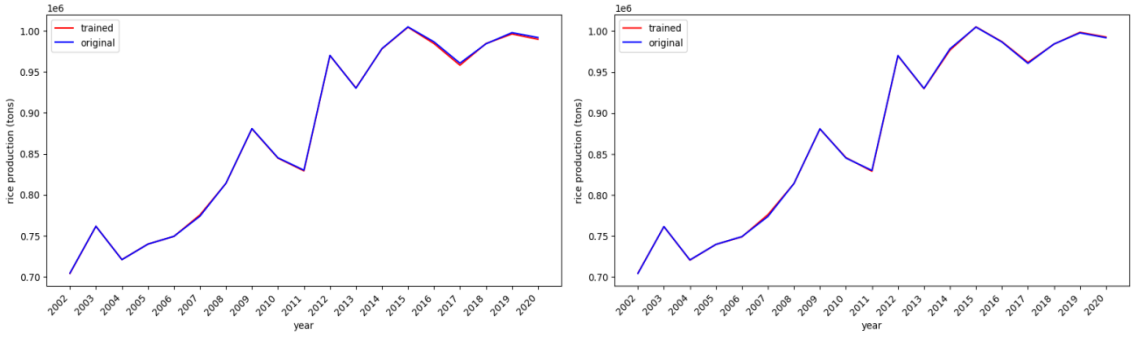

(a) Generalized Bell (b) Gaussian

Figure 4. Plot Results of Training Stage

2. Testing Stage

The testing stage used data from 2020-2022. This stage uses the membership curve and consequent parameters from the training stage results to test the untrained data.

a. Layer 1

Layer 1 output is the membership degree value obtained using the curve parameters from the training stage. Layer 1 output can be seen in **Table 13** and **Table 14** below.

Table 13. Output Layer 1 Generalized Bell Curve (Testing Stage)

$X_{1,t}$			$X_{2,t}$		$X_{3,t}$	
$\mu_{1,1}$	$\mu_{1,2}$	$\mu_{1,3}$	$\mu_{2,1}$	$\mu_{2,2}$	$\mu_{3,1}$	$\mu_{3,2}$
0.0423	0.9999	0.0449	0.1069	0.9442	0.1009	0.9999
0.0158	0.9695	0.1209	0.1539	0.8611	0.1189	0.9999

$X_{1,t}$			$X_{2,t}$		$X_{3,t}$	
$\mu_{1,1}$	$\mu_{1,2}$	$\mu_{1,3}$	$\mu_{2,1}$	$\mu_{2,2}$	$\mu_{3,1}$	$\mu_{3,2}$
0.1427	0.9110	0.0193	0.0983	0.9584	0.1174	0.9999

Table 14. Output Layer 1 Gaussian Curve (Testing Stage)

$X_{1,t}$			$X_{2,t}$		$X_{3,t}$	
$\mu_{1,1}$	$\mu_{1,2}$	$\mu_{1,3}$	$\mu_{2,1}$	$\mu_{2,2}$	$\mu_{3,1}$	$\mu_{3,2}$
0.0731	0.9971	0.0521	0.1469	0.9244	0.4092	0.9128
0.0180	0.8952	0.1369	0.2081	0.8436	0.4607	0.9455
0.2246	0.8179	0.0115	0.1344	0.9400	0.4569	0.9434

b. Layer 2

The results of firing strength at the testing stage can be seen in **Table 15** and **Table 16**.

Table 15. Output Layer 2 Generalized Bell Curve (Testing Stage)

$w_{1,t}$	$w_{2,t}$	$w_{3,t}$	⋯	$w_{10,t}$	$w_{11,t}$	$w_{12,t}$
4.5×10^{-4}	4.5×10^{-3}	4.0×10^{-3}	⋯	4.8×10^{-3}	4.2×10^{-3}	4.2×10^{-2}
2.8×10^{-4}	2.4×10^{-3}	1.6×10^{-3}	⋯	1.8×10^{-2}	1.2×10^{-2}	1.0×10^{-1}
1.6×10^{-3}	1.4×10^{-2}	1.6×10^{-2}	⋯	1.9×10^{-3}	2.7×10^{-3}	1.8×10^{-2}

Table 16. Output Layer 2 Gaussian Curve (Testing Stage)

$w_{1,t}$	$w_{2,t}$	$w_{3,t}$	⋯	$w_{10,t}$	$w_{11,t}$	$w_{12,t}$
4.4×10^{-3}	9.8×10^{-3}	2.7×10^{-2}	⋯	6.9×10^{-3}	1.9×10^{-2}	4.4×10^{-2}
1.7×10^{-3}	3.5×10^{-3}	7.0×10^{-3}	⋯	3.3×10^{-2}	6.5×10^{-2}	1.3×10^{-1}
1.3×10^{-2}	2.8×10^{-2}	9.6×10^{-2}	⋯	1.4×10^{-3}	4.9×10^{-3}	1.0×10^{-2}

c. Layer 3

The normalized firing strength, which is output of layer 3, shown in **Table 17** and **Table 18**.

Table 17. Output Layer 3 Generalized Bell Curve (Testing Stage)

$\bar{w}_{1,t}$	$\bar{w}_{2,t}$	$\bar{w}_{3,t}$	⋯	$\bar{w}_{10,t}$	$\bar{w}_{11,t}$	$\bar{w}_{12,t}$
3.6×10^{-4}	3.6×10^{-3}	3.2×10^{-3}	⋯	3.8×10^{-3}	3.4×10^{-3}	3.3×10^{-2}
2.3×10^{-4}	1.9×10^{-3}	1.2×10^{-3}	⋯	1.4×10^{-2}	9.8×10^{-3}	8.2×10^{-2}
1.3×10^{-3}	1.1×10^{-2}	1.2×10^{-2}	⋯	1.4×10^{-3}	1.7×10^{-3}	1.4×10^{-2}

Table 18. Output Layer 3 Gaussian Curve (Testing Stage)

$\bar{w}_{1,t}$	$\bar{w}_{2,t}$	$\bar{w}_{3,t}$	⋯	$\bar{w}_{10,t}$	$\bar{w}_{11,t}$	$\bar{w}_{12,t}$
2.7×10^{-3}	6.1×10^{-3}	1.7×10^{-2}	⋯	4.3×10^{-3}	1.2×10^{-2}	2.7×10^{-2}
1.0×10^{-3}	2.2×10^{-3}	4.3×10^{-3}	⋯	2.0×10^{-2}	4.1×10^{-2}	8.4×10^{-2}
8.7×10^{-3}	1.7×10^{-2}	6.0×10^{-2}	⋯	9.2×10^{-4}	3.1×10^{-3}	6.4×10^{-3}

d. Layer 4 and Layer 5

The consequent parameters at this stage use the consequent parameters from the training stage. The results of the testing stage of each membership curve with three membership functions of variable $X_{1,t}$ and two membership functions of variables $X_{2,t}$ and $X_{3,t}$ are shown in **Table 19**.

Table 19. Testing Stage Results

Year (t)	Actual Data ($t+1$)	Prediction Data ($t+1$)	
		Generalized bell	*Gaussian*
2020	961977	953165.635	936217.337

Year (t)	Actual Data ($t+1$)	Prediction Data ($t+1$)	
		Generalized bell	*Gaussian*
2021	983663	978283.914	1032424.457
2022	988185	957438.869	951952.553

The plot is used to visually determine the difference between the actual and predicted data from the training to the testing stages. The plot results for three membership functions of variable $X_{1,t}$ and two membership functions of variables $X_{2,t}$ and $X_{3,t}$ are shown in **Figure 5**. The blue line on the plot is the actual rice production data, the red line is the result of the training stage, and the yellow line is the result of the testing stage.

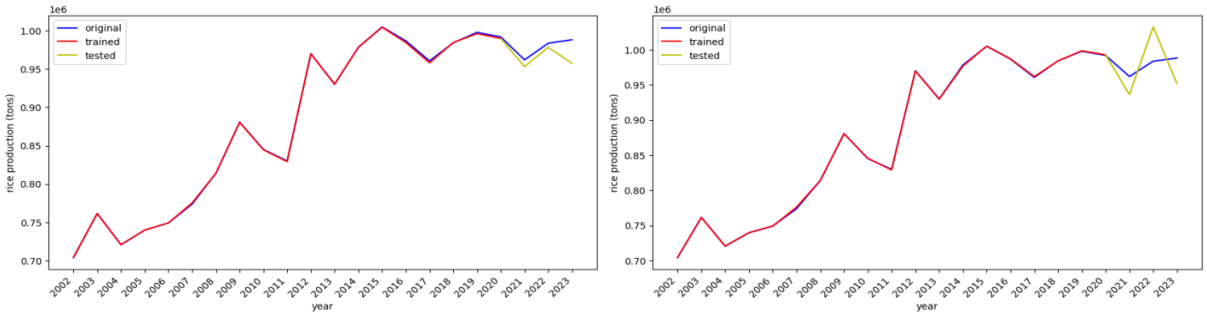

(a) Generalized Bell (b) Gaussian

Figure 5. Plot Results of Testing Stage

The plot results show that the ANFIS model with the generalized bell membership function more closely follows the shape of the actual data. It shows that the function can identify patterns in the training data and apply them to the test data.

3. Prediction Stage

This stage is used to predict rice production 2024 using input data from 2023. This prediction stage used a generalized bell function curve with three membership functions of variable $X_{1,t}$ and two membership functions of variables $X_{2,t}$ and $X_{3,t}$ because based on the results of the training and testing stages showed results that were closer to the actual results.

a. Layer 1

The output of layer 1 which is the membership degree of this stage, can be seen in **Table 20**.

Table 20. Output Layer 1 (Prediction Stage)

$X_{1,t}$			$X_{2,t}$		$X_{3,t}$	
$\mu_{1,1}$	$\mu_{1,2}$	$\mu_{1,3}$	$\mu_{2,1}$	$\mu_{2,2}$	$\mu_{3,1}$	$\mu_{3,2}$
0.9999	0.0791	0.0031	0.1099	0.9391	0.1039	0.9999

b. Layer 2

The firing strength of the prediction stage can be seen in **Table 21**.

Table 21. Output Layer 2 (Prediction Stage)

$w_{1,t}$	$w_{2,t}$	$w_{3,t}$	⋯	$w_{10,t}$	$w_{11,t}$	$w_{12,t}$
1.1×10^{-2}	1.0×10^{-1}	9.7×10^{-2}	⋯	3.4×10^{-4}	3.0×10^{-4}	2.9×10^{-3}

c. Layer 3

The normalized firing strength results can be seen in **Table 22**.

Table 22. Output Layer 3 (Prediction Stage)

$\bar{w}_{1,t}$	$\bar{w}_{2,t}$	$\bar{w}_{3,t}$	⋯	$\bar{w}_{10,t}$	$\bar{w}_{11,t}$	$\bar{w}_{12,t}$
9.1×10^{-3}	8.7×10^{-2}	7.7×10^{-2}	⋯	2.7×10^{-4}	2.4×10^{-4}	2.3×10^{-3}

d. Layer 4 and Layer 5

Like the testing stage, the prediction stage uses the consequent parameters from the training stage. The results of the prediction stage can be seen in **Table 23**. The plot results are shown in **Figure 6**. The green line represents the output of the prediction results.

Table 23. Prediction Stage Results

Year of Prediction	Prediction Data
2024	922136.8317

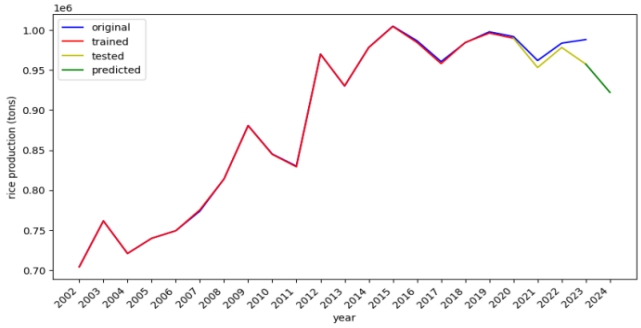

Figure 6. Plot Results of Prediction Stage

At this stage, the prediction of rice production in 2024 is 922,136.8317 tons. These results show that rice production will decrease by 66,048.17 tons from the previous year.

B. Accuracy Calculation

The accuracy of the ANFIS prediction system is calculated using Mean Absolute Percentage Error (MAPE). The error results of the training and testing stages are shown in **Table 24**.

Table 24. MAPE Results of Training and Testing Stage

Membership Function			Epoch	Generalized Bell		Gaussian	
$X_{1,t}$	$X_{2,t}$	$X_{3,t}$		*Training*	*Testing*	*Training*	*Testing*
2	2	2	100	0.034%	2.201%	0.083%	2.683%
			200	0.508%	3.978%	0.140%	2.672%
			300	0.022%	3.071%	0.037%	2.690%
2	3	3	100	0.220%	7.940%	0.265%	6.415%
			200	0.619%	6.899%	0.059%	6.866%
			300	0.088%	6.973%	0.011%	6.795%
3	2	2	100	0.080%	1.525%	0.066%	3.767%
			200	0.036%	1.593%	0.071%	3.675%
			300	0.060%	1.629%	0.078%	3.735%
3	3	3	100	0.051%	4.328%	0.038%	3.118%
			200	0.044%	4.266%	0.118%	3.076%
			300	0.049%	4.157%	0.030%	1.967%
4	3	3	100	0.073%	12.465%	0.043%	4.126%
			200	0.066%	11.123%	0.044%	5.736%
			300	0.092%	8.301%	0.050%	10.219%

The MAPE results of the training stage show that all membership functions with various epochs produce values less than 1%, while the MAPE results of the testing stage produce varying values ranging from 1.5% to 12.5%. The best ANFIS model was selected based on the smallest MAPE value from both stages. Therefore, the best model was selected with a generalized bell membership curve with three membership functions of variable $X_{1,t}$ and two membership functions of variables $X_{2,t}$ and $X_{3,t}$ with an epoch of 100.

C. Discussion

The results from the training (MAPE 0.080%) and testing (MAPE 1.525%) stages demonstrate that the optimized ANFIS model possesses a high degree of accuracy and robust generalization capabilities for predicting rice production in Jember Regency. The practical implications of this finding are significant for the Jember Regency. A reliable forecasting tool with an error rate of only ~1.5% can provide crucial advance warning to regional government bodies, such as the Department of Agriculture and Food Security. For example, the prediction of a decrease in production for 2024 (from 988,185 tons in 2023 to a predicted 922,137 tons) allows policymakers to proactively plan for potential shortfalls. This could involve measures such as adjusting import quotas, preparing farmer subsidies, or optimizing supply chain logistics to stabilize local rice prices and ensure food security. For farmers and agricultural cooperatives, such predictions, if disseminated effectively, could inform planting decisions, resource allocation (e.g., fertilizer, water), and financial planning for the upcoming season.

However, the model has limitations. Its predictions are based solely on the three input variables (rainfall, harvested area, land productivity). Rice production is a complex biological system influenced by many other factors not included in this model, such as the outbreak of pests and diseases, changes in government agricultural policy (e.g., fertilizer subsidies), and extreme, unpredictable weather events (e.g., floods or droughts not captured by annual rainfall data). Furthermore, the model assumes that the historical relationships between the inputs and output will remain stable, which may not hold true in the face of rapid climate change or technological shifts in farming.

Conclusion

The prediction of rice production in Jember Regency with Adaptive Neuro Fuzzy Inference System (ANFIS) was successfully conducted. The best model identified used generalized bell membership functions (3 functions for rainfall variables and 2 functions for harvested area variables and productivity variables) with 100 epochs and produced a predicted value of 922,136.8317 tons for 2024. The model achieved high accuracy with MAPE results of 0.080% in the training stage and 1.525% in the testing stage.

The high accuracy of the model underscores the potential of ANFIS as a valuable and reliable tool for agricultural planning and policymaking in Jember Regency. The model's ability to forecast production can aid in ensuring regional food security. Future research could focus on enhancing this prediction system. Suggestions for improvement include integrating additional data sources, such as soil quality data, information on pest and disease outbreaks, and data on government policies. Furthermore, this model's framework could be tested for its applicability to other agricultural sectors within the region or adapted for rice production prediction in other regencies with similar climates.

Acknowledgement

This research is funded by the Institute for Research and Community Service (*LP2M*) of the University of Jember through the Research Group and Community Service Grant (*Hibah KeRis-DiMas*) in 2025.

References

[1] Badan Pusat Statistik Provinsi Jawa Timur, "Produksi Padi (GKG)." Accessed: Nov. 10, 2024.

[2] S. Komatsu, K. Saito, and T. Sakurai, "Changes in production, yields, and the cropped area of lowland rice over the last 20 years and factors affecting their variations in Côte d'Ivoire," *Field Crops Res*, vol. 277, p. 108424, Mar. 2022, doi: 10.1016/j.fcr.2021.108424.

[3] A. A. Asriadi and F. Firmansyah, "The Influence of Harvested Area, Rice Consumption on Rice Crop Production in Makassar City," *Baselang*, vol. 3, no. 2, pp. 115–120, Oct. 2023, doi: 10.36355/bsl.v3i2.107.

[4] F. Mena *et al.*, "Adaptive fusion of multi-modal remote sensing data for optimal sub-field crop yield prediction," *Remote Sens Environ*, vol. 318, p. 114547, Mar. 2025, doi: 10.1016/j.rse.2024.114547.

[5] N. Chaniago, "The Effect of Rainfall on Rice Production and Productivity in Percut Sei Tuan District, Deli Serdang Regency, North Sumatra," *Agriland*, vol. 11, no. 3, pp. 130–136, 2023.

[6] H. R. Bedane, K. T. Beketie, E. E. Fantahun, G. L. Feyisa, and F. A. Anose, "The impact of rainfall variability and crop production on vertisols in the central highlands of Ethiopia," *Environmental Systems Research*, vol. 11, no. 1, p. 26, Dec. 2022, doi: 10.1186/s40068-022-00275-3.

[7] M. Joseph, S. Moonsammy, H. Davis, D. Warner, A. Adams, and T. D. Timothy Oyedotun, "Modelling climate variabilities and global rice production: A panel regression and time series analysis," *Heliyon*, vol. 9, no. 4, p. e15480, Apr. 2023, doi: 10.1016/j.heliyon.2023.e15480.

[8] S. Jeong, J. Ko, J. Ban, T. Shin, and J. Yeom, "Deep learning-enhanced remote sensing-integrated crop modeling for rice yield prediction," *Ecol Inform*, vol. 84, p. 102886, Dec. 2024, doi: 10.1016/j.ecoinf.2024.102886.

[9] D. A. Korzhakin and E. Sugiharti, "Implementation of Genetic Algorithm and Adaptive Neuro Fuzzy Inference System in Predicting Survival of Patients with Heart Failure," *Scientific Journal of Informatics*, vol. 8, no. 2, pp. 251–257, Nov. 2021, doi: 10.15294/sji.v8i2.32803.

[10] S. Radfar, H. Koosha, A. Gholami, and A. Amindoust, "A neuro-fuzzy and deep learning framework for accurate public transport demand forecasting: Leveraging spatial and temporal factors," *J Transp Geogr*, vol. 126, p. 104217, Jun. 2025, doi: 10.1016/j.jtrangeo.2025.104217.

[11] S. S. Tabrizi and N. Sancar, "Prediction of Body Mass Index: A comparative study of multiple linear regression, ANN and ANFIS models," *Procedia Comput Sci*, vol. 120, pp. 394–401, 2017, doi: 10.1016/j.procs.2017.11.255.

[12] N. S. Mohd Ali *et al.*, "Power peaking factor prediction using ANFIS method," *Nuclear Engineering and Technology*, vol. 54, no. 2, pp. 608–616, Feb. 2022, doi: 10.1016/j.net.2021.08.011.

[13] L. Wang and S. Pang, "An Implementation of the Adaptive Neuro-Fuzzy Inference System (ANFIS) for Odor Source Localization," in *2020 IEEE/RSJ International Conference on Intelligent Robots and Systems (IROS)*, IEEE, Oct. 2020, pp. 4551–4558. doi: 10.1109/IROS45743.2020.9341688.

[14] M. Achite, E. Gul, N. Elshaboury, M. Jehanzaib, B. Mohammadi, and A. Danandeh Mehr, "An improved adaptive neuro-fuzzy inference system for hydrological drought prediction in Algeria," *Physics and Chemistry of the Earth, Parts A/B/C*, vol. 131, p. 103451, Oct. 2023, doi: 10.1016/j.pce.2023.103451.

[15] Z. Zulfauzi, B. Santoso, M. A. S. Arifin, and S. Nuraisyah, "Implementation of Adaptive Neuro-Fuzzy Inference System (Anfis) Method on Rice Price Prediction in Lubuklinggau City," *JURNAL TEKNOLOGI DAN OPEN SOURCE*, vol. 4, no. 2, pp. 260–269, Dec. 2021, doi: 10.36378/jtos.v4i2.1847.

[16] H. Haviluddin, H. S. Pakpahan, N. Puspitasari, G. M. Putra, R. Y. Hasnida, and R. Alfred, "Adaptive Neuro-Fuzzy Inference System for Waste Prediction," *Knowledge Engineering and Data Science*, vol. 5, no. 2, p. 122, Dec. 2022, doi: 10.17977/um018v5i22022p122-128.

[17] W. Suparta and A. A. Samah, "Rainfall prediction by using ANFIS times series technique in South Tangerang, Indonesia," *Geod Geodyn*, vol. 11, no. 6, pp. 411–417, Nov. 2020, doi: 10.1016/j.geog.2020.08.001.

[18] S. D. Barewar, P. S. Kalos, B. Bakthavatchalam, M. Joshi, S. Patil, and M. Sonekar, "Analysis and prediction of thermo-physical properties in water-based MWCNT-ZnO hybrid nanofluids using ANN and ANFIS models," *International Journal of Thermofluids*, vol. 27, p. 101159, May 2025, doi: 10.1016/j.ijft.2025.101159.

[19] P. Mottahedin, B. Chahkandi, R. Moezzi, A. M. Fathollahi-Fard, M. Ghandali, and M. Gheibi, "Air quality prediction and control systems using machine learning and adaptive neuro-fuzzy inference system," *Heliyon*, vol. 10, no. 21, p. e39783, Nov. 2024, doi: 10.1016/j.heliyon.2024.e39783.

[20] B. Khoshnevisan, S. Rafiee, M. Omid, and H. Mousazadeh, "Development of an intelligent system based on ANFIS for predicting wheat grain yield on the basis of energy inputs," *Information Processing in Agriculture*, vol. 1, no. 1, pp. 14–22, Aug. 2014, doi: 10.1016/j.inpa.2014.04.001.

[21] A. Kamsyakawuni, W. Sholihah, and A. Riski, "Prediction System For The Amount Of Sugar Production Using Adaptive Neuro-Fuzzy Inference System," *BAREKENG: Jurnal Ilmu Matematika dan Terapan*, vol. 18, no. 4, pp. 2597–2610, Oct. 2024, doi: 10.30598/barekengvol18iss4pp2597-2610.

[22] X. Han, F. Liu, X. He, and F. Ling, "Research on Rice Yield Prediction Model Based on Deep Learning," *Comput Intell Neurosci*, vol. 2022, pp. 1–9, Apr. 2022, doi: 10.1155/2022/1922561.

[23] M. B. Gorzalczany, *Computational Intelligence Systems and Applications: Neuro-Fuzzy and Fuzzy Neural Synergisms*, vol. 86. Heidelberg: Physica-Verlag, 2002.

[24] J.-S. R. Jang, C.-T. Sun, and E. Mizutani, *Neuro-Fuzzy and Soft Computing: A Computational Approach to Learning and Machine Intelligence*. New Jersey: Prentice Hall, 1997.

[25] R. Abdi, G. Shahgholi, V. R. Sharabiani, A. R. Fanaei, and M. Szymanek, "Prediction compost criteria of organic wastes with Biochar additive in in-vessel composting machine using ANFIS and ANN methods," *Energy Reports*, vol. 9, pp. 1684–1695, Dec. 2023, doi: 10.1016/j.egyr.2023.01.001.

[26] C. T. . Lin and C. S. G. . Lee, *Neural fuzzy systems : a neuro-fuzzy synergism to intelligent systems*. Prentice Hall PTR, 1996.

[27] P. Xu, U. F. Alqsair, and A. S. El-Shafay, "Prediction of gas fraction in wastewater treatment with ANFIS method for different height of single sparger location," *Environ Technol Innov*, vol. 26, p. 102350, May 2022, doi: 10.1016/j.eti.2022.102350.

[28] S. Kim and H. Kim, "A new metric of absolute percentage error for intermittent demand forecasts," *Int J Forecast*, vol. 32, no. 3, pp. 669–679, Jul. 2016, doi: 10.1016/j.ijforecast.2015.12.003.

[29] A. de Myttenaere, B. Golden, B. Le Grand, and F. Rossi, "Mean Absolute Percentage Error for regression models," *Neurocomputing*, vol. 192, pp. 38–48, Jun. 2016, doi: 10.1016/j.neucom.2015.12.114.

[30] A. Binbusayyis and M. Sha, "Energy consumption prediction using modified deep CNN-Bi LSTM with attention mechanism," *Heliyon*, vol. 11, no. 1, p. e41507, Jan. 2025, doi: 10.1016/j.heliyon.2024.e41507.

[31] R. K. C. Chan, J. M.-Y. Lim, and R. Parthiban, "Long-term traffic speed prediction utilizing data augmentation via segmented time frame clustering," *Knowl Based Syst*, vol. 308, p. 112785, Jan. 2025, doi: 10.1016/j.knosys.2024.112785.

[32] P.-Y. Chen, C.-C. Chen, C. Kang, J.-W. Liu, and Y.-H. Li, "Soil water content prediction across seasons using random forest based on precipitation-related data," *Comput Electron Agric*, vol. 230, p. 109802, Mar. 2025, doi: 10.1016/j.compag.2024.109802.

[33] M. Jiang *et al.*, "Multistep prediction for egg prices: An efficient sequence-to-sequence network," *Egyptian Informatics Journal*, vol. 29, p. 100628, Mar. 2025, doi: 10.1016/j.eij.2025.100628.

[34] T. Meggs, "anfis." Accessed: Dec. 13, 2024.